

SEA SURFACE SALINITY FROM SPACE: SCIENCE GOALS AND MEASUREMENT APPROACH

C.J. Koblinsky¹, P. Hildebrand¹, Y. Chao², A. deCharon⁷, W. Edelstein², G. Lagerloef³, D. LeVine¹, F. Pellerano¹, Y. Rahmat-Samii⁶, C. Ruf⁴, F. Wentz⁵, W. Wilson², and S. Yueh²

1 – NASA/Goddard, 2 – NASA/JPL, 3 – Earth and Space Research, Inc., 4 – Univ. Michigan,
5 – Remote Sensing Systems, Inc., 6 – UCLA, 7 – Bigelow Labs Ocean Sciences

1. SALINITY SCIENCE GOALS

The salinity of the ocean surface (Fig. 1) ranges from about 32 to 38 parts per thousand, reflecting the input of fresh water from precipitation, melting of ice and river runoff, the loss of water through evaporation, and the mixing and circulation of ocean surface water with deep water below. Globally, the sea surface salinity (SSS) is at a minimum near the equator (where there is considerable precipitation) and in polar regions (due to the melting of ice), and is enhanced in mid latitudes (where there is reduced precipitation and enhanced evaporation).

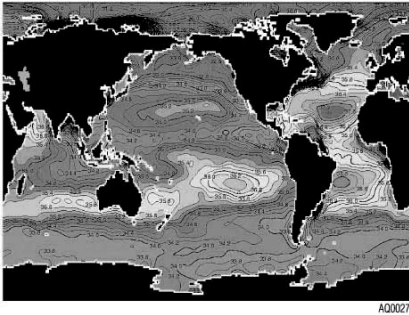


Fig.1. The estimated annual mean global SSS field from historical data, with salinities ranging from 32 (dark) to 37 (light). (After Levitus, et al, 1998)

Understanding the variability of oceanic salinity is extremely important to the full understanding of the relationship between ocean circulation and climate. This is because ocean buoyancy is a roughly equal function of sea water temperature and salinity. At the present time, only the sea surface temperature is adequately measured on a global scale. Additional inputs to ocean circulation include surface wind stress, and internal forces, including coriolis, frictional and waves. Global measurement of oceanic salinity will therefore enable understanding the buoyancy forcing of oceanic circulation.

1. Corresponding author address: Peter H. Hildebrand, NASA Goddard, Greenbelt, MD, 20771; peter.hildebrand@gsfc.nasa.gov

Improved understanding of the oceanic buoyancy field will improve our understanding of seasonal to interannual changes in ocean circulation and the feedback between ocean circulations and its feedback to the climate.

The depiction of SSS shown in Fig. 1 is based on averaging extensively over space and time (many years) and resolves only the largest, basin-scale salinity patterns. The knowledge of seasonal-to-interannual variability is much more poorly observed. This is because the actual measurements of SSS (Fig. 2) are limited; over 42% of the ocean has never been observed and for over 88% of the ocean there are fewer than 10 measurements over the past 125 years (Levitus, et al, 1998).

Number of Observations by 1° Square

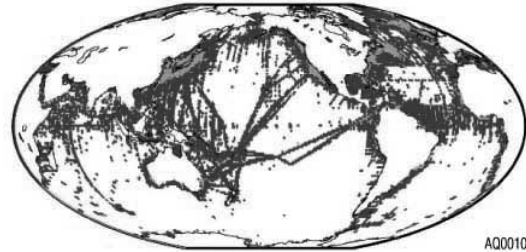


Fig. 2. Salinity observation density over past 125 years (Courtesy of F. Bingham based upon Levitus et al, 1998)

The salinity measurements that do exist suggest that at any one location the salinity varies by <1 psu, and the variability is frequently only a few tenths of a psu. Although there are only sketchy measurements, this same result comes from numerical modeling, the analysis of the underlying variability of salinity measurements at single locations, the observations of salinity anomalies (e.g. Dickson, et al, 1988; Belkin et al, 1998), studies of the effects of rainfall or runoff (e.g. Cronin and McPhaden, 1999) or from studies of seasonal to interannual salinity variability (e.g. Dessier and Donguy, 1994; Donguy and Meyers, 1996; Large and Nurser, 1997; Delcroix, 1998; Delcroix and McPhaden, 2001).

To provide global SSS measurements and meet these scientific challenges, we have proposed the Aquarius mission to the NASA Earth System Science Pathfinder Program. Aquarius measurements are designed to address

NASA Earth Science Enterprise goals concerning the global water cycle and the links between global ocean circulations to climate change. This will be done through providing the first ever observations of the global SSS basic state, plus observation of seasonal to interannual changes over the life of the program. The science goals of Aquarius are therefore to: a) provide the first, global mapping of the complete oceanic SSS field, b) to better describe the global thermohaline circulation, c) to improve understanding of the tropical ocean-climate feedback such as el Niño, and d) to facilitate investigations of the freshwater budget component of coupled ocean-atmosphere models. The temporal and spatial scales of important oceanographic phenomena and the measurement resolution capabilities of Aquarius are illustrated in Fig. 3. Also shown are the estimated amplitudes of the salinity variability for these phenomena in psu.

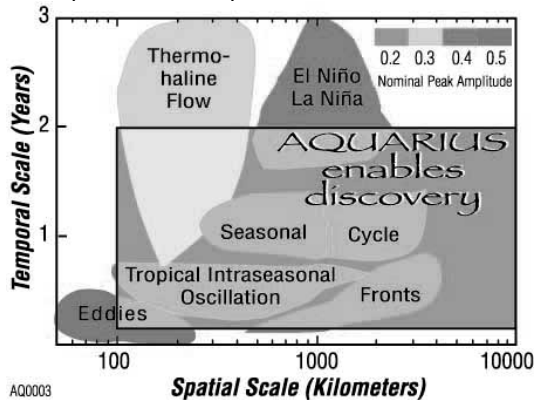


Fig. 3. The spatial and temporal scales of important oceanographic phenomena.

2. SALINITY MEASUREMENT GOALS

To meet the science goals, the Aquarius satellite must provide measurements of SSS to 0.2 – 0.4 psu, at a spatial sampling interval of 100 to 200 km and at a temporal sampling interval of 1 month. As illustrated in Figs 1 and 3, salinity measurements accurate to 0.2 psu are expected to be entirely accurate for the Aquarius science goals, and even measurements accurate to 0.3-0.5 psu would provide a major improvement in the current knowledge of SSS.

The Aquarius Salinity Measurement Satellite is therefore designed to measure global SSS with ~100 km resolution, every 8 days and will characterize salinity variability over a two year lifetime. With this coverage, salinity will be measured to an accuracy of ~0.2 psu in the tropics and ~0.3 psu at high latitudes, and over the range from 32 to 38 psu. The measurement domain will include the open ocean more than 150 km from coastal and sea ice boundaries.

3. RADIOMETRIC MEASUREMENT OF SALINITY

The underlying physics of salinity remote sensing from satellites is based on the sensitivity of the brightness temperature of sea water, T_b , to SSS and sea surface temperature, T_s . At microwave frequencies. T_b is related to SSS and T_s by the relation $T_b = e \cdot T_s$, where e is the emissivity of the sea surface, itself a function of SSS and T_s . This sensitivity is strongest in the frequency range from 0.5 to 1.5 GHz; the protected frequency band at 1.4 GHz (L-band) has been selected for Aquarius. For typical ranges of SSS and T_s over the open oceans, the T_b at L-band has a range of about 4-6K. The sensitivity of T_b to changes in SSS vs. T_s (Fig. 4) is greatest in warm water (0.7K/psu at 30°C) and least in cold (0.3K/psu at 0°C).

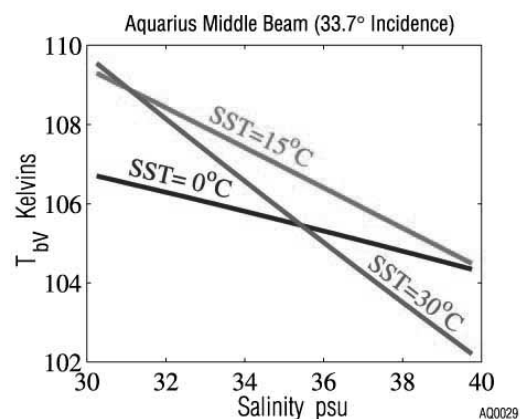


Fig. 4. Sensitivity of sea surface brightness temperature to T_s and salinity.

Measurement of salinity with this technique is complicated by several factors, the largest of which is the significant effect of sea surface roughness on microwave emission (Table 1). Sea surface roughness effects can produce a ΔT_b of up to ~5K, for very a rough sea surface. This effect dictates the need for an accurate means of measuring the sea surface roughness, which also must be accomplished simultaneously with the T_b measurements, due to the short time scale of sea surface wind variability.

Other contributions to the measured T_b at L-band include galactic emissions (ΔT_{bGAL} of ~2K), atmospheric emissions (ΔT_{bATM} ~2.4-2.8K), and emission from water vapor and cloud liquid water (both have a small effect on T_b). Additionally, the Faraday rotation of the polarized microwave emissions as the radiation passes through the ionosphere, needs to be corrected for. (Although there is no effect on $(T_{bV}+T_{bH})$, the individual T_{bV} and T_{bH} measurements can change by up to 5K.

The retrieval algorithm for SSS consists of two parts; a) evaluation of T_b at the sea surface and b) retrieval of SSS from T_b . The Aquarius instrument provides T_b at the satellite. Radiative transfer models allow correction for up- and down-welling emission from the atmosphere,

atmospheric and ionospheric attenuation and Faraday rotation. Down-welling galactic emissions are also taken into account using accurate maps. With these corrections, plus knowledge of the T_s and surface roughness, salinity can be calculated from T_b . Residual corrections to these data analysis algorithms will be carried out in a series of steps that have already begun with a series of aircraft test programs, plus laboratory and model developments. Algorithm refinement will continue with end-to-end simulation of the data algorithm system using ocean and atmospheric models, plus field experiment data. Finally, instrument calibration will include three major thrusts including deep space calibration maneuvers, detailed calibration corrections using highly accurate in-situ measurements of SSS, T_s , winds and roughness from buoy networks, plus error reduction approaches (e.g. Ruf, 2000; Wentz et al, 2000) that have been proven to be effective approaches to error reduction on other satellite data analysis systems.

4. AQUARIUS MEASUREMENT APPROACH

The first radiometric observations of salinity from space used an L-band radiometer on Skylab in the mid 1970s. Early design studies (e.g. Swift and McIntosh, 1983) detailed the conceptual design approach, and the required microwave emission model (Klein and Swift, 1977). Since then, aircraft instruments and flight programs have addressed the technical details of building the highly accurate L-band radiometer required to accurately measure SSS (Fig 5 and LeVine, et al, 1998 and 2001; Wilson, et al, 2001a,b). Based on these developments, the state of technology is now sufficient to produce an accurate L-band radiometer-scatterometer system that can be coupled with a planned global array of in situ salinity observations to provide the needed level of measurement accuracy.

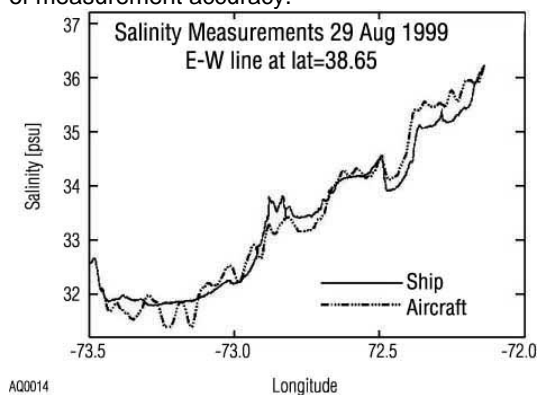


Fig. 5. Comparison of L-band radiometer and ship salinity measurements (Levine et al 1998).

The Aquarius design (Fig. 6) includes V- and H-polarized, 1.413 GHz radiometers and a 1.2 GHz

scatterometer. A 3 m offset paraboloid reflector will be illuminated by three separate feeds to produce three beams with a 5.5° beamwidth and beam efficiencies of 95%. Each beam will include V- and H-polarization radiometers, plus an H-polarization scatterometer sampling of the ocean surface. The three beams will have incidence angles of 23.3° , 33.7° , and 41.7° . The resultant three-beam swath width of 250 km will give complete global coverage in 8 days and enough samples within a month to meet the accuracy requirement through averaging (see Table 1 and Yueh et al, 2001). The orbit will be a 6am/6pm orbit, with the beams directed toward the dark side of the earth in order to avoid reflected solar radiation.



Fig. 6. Aquarius design concept showing the three feeds, the main reflector and the solar array.

The *Aquarius* instrument design was selected to meet the science needs within the constraints of measurement accuracy, spatial and temporal sampling requirements, global ocean coverage, and project risk and cost. The radiometer/scatterometer design is based on the lessons from integration of similar systems on the PALS systems (Wilson, et al, 2001a,b) and on the Advanced Water Vapor Radiometer (AWVR, Randa, et al, 2000) which has demonstrated radiometer stability of $\sim 0.05K$ over 30 day time scales; more than a factor of two better than required for *Aquarius*.

5. REFERENCES

- Belkin, I.M., S. Levitus, J. Antonov, and S.-A. Malmberg, 1998: Great Salinity Anomalies in the North Atlantic. *Prog. Oceanogr.* **41**, 1-68.
- Cronin, M.F., and M.J. McPhaden, 1999: Diurnal cycle of rainfall and surface salinity in the western Pacific warm pool, *Geophys. Res. Letters*, **26**, 3465-3468.
- Delcroix, T., 1998: Observed surface oceanic and atmospheric variability in the Tropical Pacific at seasonal and ENSO time scales: a tentative overview., *J. Geophys. Rev.*, **103**, 18611-18633.

- Delcroix, T. and M.J. McPhaden, 2001: On SSS changes in the western Pacific warm pool during the 1992-1999 ENSO events., *J. Geophys. Res.*, (submitted)
- Dessier, A. and J.-R. Donguy, 1994: The SSS in the tropical Atlantic between 10S and 30N—seasonal and interannual variations (1997-1989), *Deep Sea Res.*, **41**, 81-100.
- Dickson, R.R., J. Meincke, S.-A. Malmberg and A.J. Lee, 1988: The Great Salinity Anomaly in the northern north Atlantic, 1968-1982, *Prog. Oceanogr.* **20**, 103-151.
- Donguy, J.-R. and G. Meyers, 1996: Seasonal variations of sea-surface salinity and temperature in the tropical Indian Ocean. *Deep Sea Res.*, **43**, 117-138.
- Levitus, S., T.P. Boyer, M.E. Conkright, T. O'Brien, J. Antonov, C. Stephens, L. Statoplos, D. Johnson and R. Gelfeld, 1998: NOAA/NESDIS 18, World Ocean Database, **1**, 346pp.
- Klein, L. and C. Swift, 1977: An improved model for the dielectric constant of sea water at microwave frequencies. *IEEE Trans. Antennas Propag.* **AP-25**, 104-111.
- Large, W. and A. Nurser, 2001: Ocean surface water mass transformation. Eds.: J. Church and J. Gould. *Ocean Circulation and Climate*, 317-336.
- LeVine, D., M. Kao, R. Garvine and T. Saunders, 1998: Remote sensing of ocean salinity: Results from the Delaware coastal current experiment., *J. Atmos. Ocean. Technol.*, **15**, 1478-1484.
- LeVine, D., C. Koblinsky, F. Pellerano, G. Lagerloef, Y. Chao, S. Yueh and W. Wilson, 2001: The measurement of salinity from space: Sensor concepts. *IGARSS 2001*, Sydney, Australia, July 2001.
- Randa, J., L. Dunleavy and L. Terrell, 2000: Stability measurements on noise sources, *IEEE Trans. Inst. Meas.*, **50**, 368-372.
- Ruf, C., 2000: Detection of calibration drifts in spaceborne microwave radiometers using a vicarious cold reference, *IEEE Trans. Geosci. Remote Sens.*, **38**, 44-52.
- Swift, C. and R. McIntosh, 1983: Considerations for microwave remote sensing of ocean surface salinity, *IEEE Trans. Geosci. Remote Sens.*, **21**, 480-491.
- Wentz, F., C. Gentemann, D. Smith, and D. Chelton, 2000: Satellite measurement of sea surface temperature through clouds, *Science*, **288**, 847-850.
- Wilson, W, S. Yueh, S. Dinardo, S. Chazanoff, A. Kitiyakara and F. Li, 2001a: Passive-active L- and S-band (PALS) microwave sensor for ocean salinity and soil moisture measurements, *IEEE Trans. Geosci. Remote Sens.*, **39**, 1039-1048.
- Wilson, W, S. Yueh, f. Li, S. Dinardo, Y. Chao, C. Koblinsky, G. Lagerloef, and S. Howden, 2001b: Ocean salinity remote sensing with the JPL Passive/Active L-/S-band (PALS) microwave instrument. *IGARSS 2001*, Sydney, Australia, July 2001.
- Yuan, X., and L. Talley, 1992: Shallow salinity minima in the north Pacific, *J. Geophys. Oceanogr.*, **22**, 1302-1316.
- Yueh, S., R. West, W. Wilson, F. Li, E. Njoku, and Y. Rahmat-Samii, 2001: Error sources and feasibility for microwave remote sensing of SSS, *IEEE Trans. Geosci. Remote Sensing*, **39**, 1049-1060.

Table 1. Aquarius error analysis for sea surface salinity retrieval algorithm using T_{bv} .

Geophysical Parameter	Impact on T_{bv}	Supplementary Data Set For Correction	Residual Error in T_{bv} (K)	Salinity Error at mid Latitudes
Surface Roughness	< 5 K	Scatterometer ($\pm 2\%$)	0.10	0.18
SST	$\pm 0.14K/ 1^\circ C$ SST	NCEP SST products ($\pm 0.5^\circ C$)	0.07	0.00
Dry Air	2.4-2.8K	NCEP air temperature ($\pm 2^\circ C$) and pressure ($\pm 5hPa$)	0.07	0.13
Cloud Liquid Water	<0.1K	Operational integrated columnar water vapor ($\pm 0.15mm$ water)	0.04	0.07
Water Vapor	<0.01K	NA	0.005	0.01
Faraday Rotation	<5K	Polarimetric radiometer measurements provide $\leq \pm 0.2K$ error	0.02	0.04
Galactic	<2K + 3K bkgnd.	Sky survey with 1% accuracy	0.02	0.04
RSS of total geophysical error per observation			0.16	0.26
Radiometer calibration stability per observation			0.18	0.33
Radiometer $NE\Delta T$ per observation			0.06	0.10
RSS of total error per observation			0.25	0.43
Average number of monthly Aquarius observations per 100 km grid cell				9
Aquarius monthly average accuracy, assuming $1/\sqrt{n}$ improvement (psu)				0.14